Fermilab FERMILAB-CONF-07-416-APC   August 2007

MARS15 CODE IN ACCELERATOR APPLICATIONS

Noriaki Nakao and Nikolai V. Mokhov

Fermi National Accelerator Laboratory (Fermilab): MS220, P.O.Box 500, Batavia, IL 60510, USA
E-mail:nakao@fnal.gov

MAD-MARS Beam-Line Builder (MMBLB) is a tool that helps MARS15 build models of accelerator lattices and beam lines using the MAD-generated optics descriptions. This mode is especially powerful in beam loss, collimation, backgrounds and shielding studies at the existing and new accelerators and beam transport lines. Many applications works using this tool have been performed such as Main Injector and Tevatron at Fermilab, Large Hadron Collider (LHC) at CERN, 3GeV-RCS at J-PARC, and International Linear Collider (ILC).

The paper describes the basics of MMBLB using various simple beam-line examples to help users understand better. Also, focusing on realistic studies of collimation and shielding, a few representative MMBLB applications are described here especially for a 350-m proton ring of J-PARC 3GeV-RCS and a 1.6-km long 250-GeV positron beam line of the ILC beam delivery system (BDS).

MARS15 CODE IN ACCELERATOR APPLICATIONS

Noriaki Nakao and Nikolai V. Mokhov

Fermi National Accelerator Laboratory (Fermilab): MS220, P.O.Box 500, Batavia, IL 60510, USA
E-mail:nakao@fnal.gov

MAD-MARS Beam-Line Builder (MMBLB) is a tool that helps MARS15 build models of accelerator lattices and beam lines using the MAD-generated optics descriptions. This mode is especially powerful in beam loss, collimation, backgrounds and shielding studies at the existing and new accelerators and beam transport lines. Many applications works using this tool have been performed such as Main Injector and Tevatron at Fermilab, Large Hadron Collider (LHC) at CERN, 3GeV-RCS at J-PARC, and International Linear Collider (ILC).

The paper describes the basics of MMBLB using various simple beam-line examples to help users understand better. Also, focusing on realistic studies of collimation and shielding, a few representative MMBLB applications are described here especially for a 350-m proton ring of J-PARC 3GeV-RCS and a 1.6-km long 250-GeV positron beam line of the ILC beam delivery system (BDS).

I. INTRODUCTION

MARS code [1] is a Monte Carlo code for electro-magnetic hadron cascade transport, which has been widely used for simulations of beam-induced energy deposition, radiation dose and particle-flux estimation in accelerator applications. MAD-MARS Beam Line Builder (MMBLB) [2,3,4] is one of the key elements of this code, which can make it easier to describe multiply repeated beam-line elements with a bent beam line by dipole magnet using the OPTICS data file of the MAD code [5].

This paper presents basics of MMBLB of the MARS15 code, and recent studies of collimation and shielding using MMBLB for bent and complicated beam lines of a few accelerator projects. All the plots were generated using the powerful MARS15 GUI [1].

II. MAD-MARS BEAM LINE BUILDER (MMBLB)

In MMBLB, the beam-line elements and tunnel are prepared in different coordinates for the user's flexibility and convenience. Elements such as beam pipe, quadrupole, dipole magnet and collimator are made in each individual local (relative) coordinate in the beam-orbit axis from z=0 to z=L as shown in Fig.1. The L is defined in the OPTICS file. On the other hand, outside structure geometry such as the tunnel shielding wall, room and dirt are prepared in the global (absolute) coordinate as shown in Fig.2 where the actual Monte-Carlo simulation is carried out.
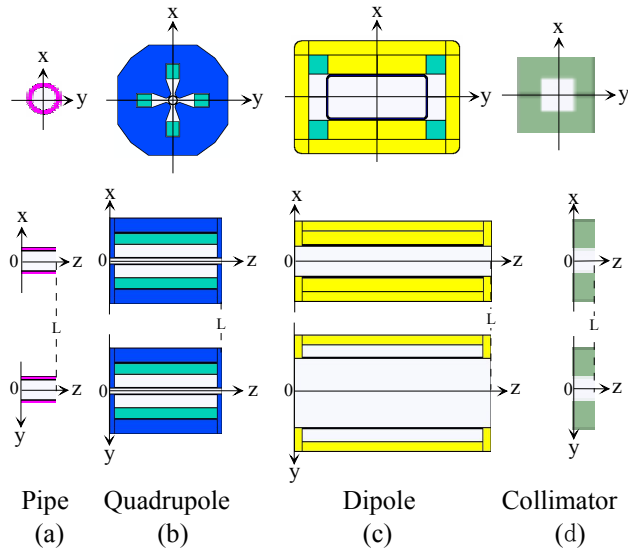

Fig.1. Cross-sectional, vertical and horizontal plane views of beam-line element geometries for (a)beam pipe, (b)quadrupole magnet, (c)dipole magnet and (d)collimator in their individual local coordinates for MMBLB.
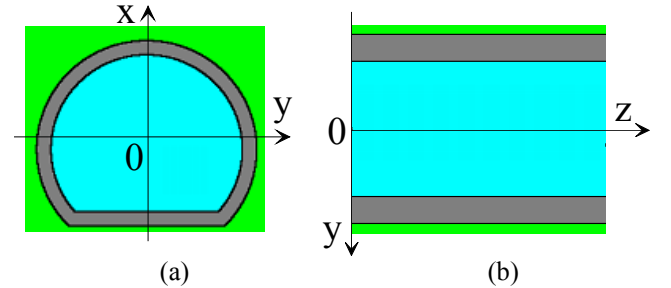

Fig. 2. Tunnel structure in the global coordinate. (a)cross-sectional view and (b)horizontal plane view.

Each element set contains information of name, material, magnetic field and volume. Those are defined in the user subroutines named by the user like *_func listed below, and these are registered in a set of one element in subroutine BLGINIT, which is called at the initialization stage.

```
name_func         : assign TYPE and NAME
name_func         : initialization and user definition
geo_func          : describe geometry
mat_func          : assign materials to regions
field_func        : describe magnetic field
vol_func          : define volumes in regions
zonename_func : define name for each zone
```

The OPTICS file contains length, bending angle and magnetic-field parameters of each beam-line element. A simple example of the OPTICS list (from 3rd line) is given below. One element is given in one line.

Keyword	TYPE	NAME	SumL [m]	L [m]	Bend k0L [rad]	Q k1L	Sx k2L	Oc k3L	Tilt [rad]

-----(start OPTICS file)---									
"DRIFT"	"DL10"	"DPC1"	1.0	1.0	0.	0.	0.	0.	0.
"SBEND"	"H20"	"BPC1"	4.0	3.0	2.4E-4	0.	0.	0.	0.
"DRIFT"	"DL10"	"DPC2"	20.0	16.0	0.	0.	0.	0.	0.
"SBEND"	"H20"	"BPC1"	23.0	3.0	2.4E-4	0.	0.	0.	0.
"DRIFT"	"DL10"	"DPC3"	20.5	16.0	0.	0.	0.	0.	0.
:									
-----(end OPTICS file)---									

```
Keyword: Specific MAD 15 keywords are allowed
TYPE    : Element type defined by user in subroutine name_func
NAME    : Specific name defined by user in subroutine name_func
SumL    : Sum of L (ignored in MARS)
L       : Length (m) of the element
k0L     : Bending angle (rad) of a dipole magnet
k1L     : Factor for gradient of quadrupole magnet
k2L     : Factor for gradient of sextupole magnet
k3L     : Factor for gradient of octupole magnet
TILT    : Roll angle (rad) of the element around s-axis (orbit axis)
```
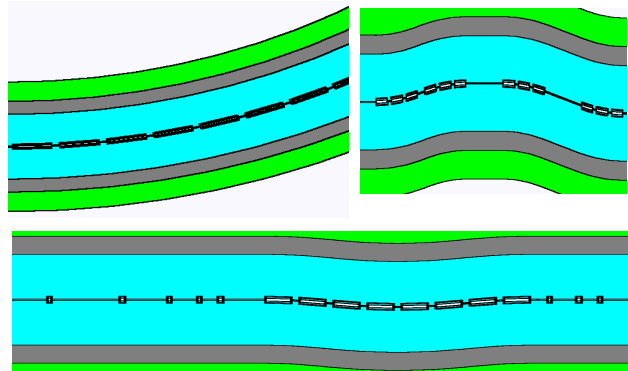

Fig. 3. Various beam lines with tunnels with the different OPTICS using the same beam-line elements.

The element set which has the same combination of TYPE and NAME is selected as a beam line component in the location, and length, angle and field parameters are given by the OPTICS. TILT is roll angle which makes it possible to describe 3D beam line. A positive angle forms a right-hand screw with the orbit axis.

The corresponding element appears in the global coordinate in the order that the element appears in the list of the OPTICS. The detailed magnetic-field maps for quadrupole, sextupole and octupole magnets to focus or defocus the beam are defined or read in a user subroutine. The absolute intensities of all magnets are given by the field parameters (i.e. k0L) in the OPTICS to adjust the field map.

Fig.3 shows three beam-line tunnels in the global coordinate defined by three different the OPTICSs using the same beam-line element sets. Tunnel shape can be independent of the beam-line bending as shown in Fig.4(a) which is useful for a straight tunnel. On the other hand, a tunnel shape can follow a beam-line bending shape as shown in Fig.4(b) which is useful for a ring-type accelerator or a bending tunnel.

Two types of dipole magnets can be selected as shown in Fig. 5. "SBEND" is a fan-shaped geometry with different volumes between inner and outer parts in spite of the symmetric cross section. "RBEND" is a straight dipole which is slightly shifted outward with a wider aperture to avoid beam interaction at the beam pipe. Definitions of length (L) of dipole for SBEND and RBEND are given by arc and chord as shown in Fig.5.
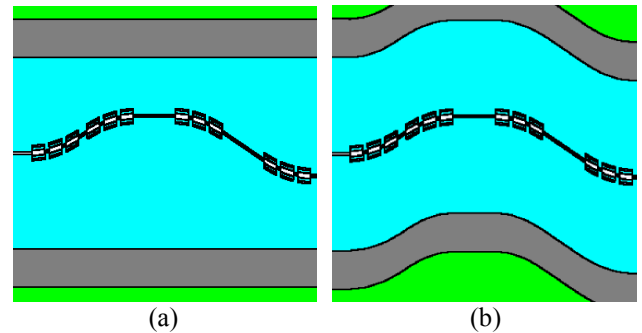

(a)	(b)

Fig.4. Two beam lines described with the same OPTICS with tunnel shape (a)independent of or (b)following the beam line shape.
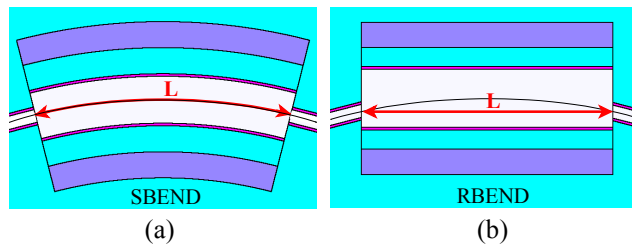

(a)	(b)

Fig.5. Horizontal view of two types of dipole magnet, (a)SBEND and (b)RBEND. Length (L) definitions are also indicated in red arrow.

III. J-PARC 3GeV-RCS

One of the earliest applications of MMBLB was a simulation for the J-PARC 3GeV-RCS ring [6, 7]. As shown in Fig.6, an entire-triangle ring of 350-m circumference was described by MMBLB. Beam line components such as magnet and collimator are described along with the MAD OPTICS file.

Fig.7 shows a vertical view of the region from the injection through collimation section with a 2-story structure tunnel. A collimator with massive shielding and beam-line upper local-shielding, which consists of iron and concrete, were prepared as a beam-line element and were used several times in this region as shown in the figure. A local shield in the injection, which consists of iron and concrete in a sandwich structure, was described as a part of the tunnel in the global coordinate. Concrete thicknesses of the roof and floor were designed to satisfy the dose limit at the soil boundary based on the ground-water activity limit.

Flux-detector cells of about 1-m interval were located at the shielding wall and soil region at several depths as shown in Figs.7 and 8, and prompt dose rates were calculated. Fig.8 shows a top view of the first arc section with several dipole magnets. The dipole used here is a SBEND type. The volumes of the detector cells in the shielding of the SBEND region vary between inner- and outer-shield of the ring, and this effect was also considered in the volume calculation.

Fig.9 shows magnetic field images for dipole- and quadrupole-magnets. Field maps were given by POISSON[8] calculations. Beam orbit tests were performed with 400-MeV and 3-GeV protons starting from a 0-m foil position, and these protons arrive at the same position after running through the entire ring. This beam test indicates that the magnetic fields are accurate at all magnets, and the fields worked properly.

Fig.10 shows one of the simulation results for prompt-dose rate at the detector cells of Fig.7. Dose-rate distributions in various depths of shielding at floor and sub-tunnel in the region from the injection through collimation section are shown in the figure. The source term used in the simulation, which is the beam-loss distribution of 400-MeV proton-beam halo simulated by STRCUT code [9], is also shown in the top of Fig.10.

Prompt dose limits at the soil boundary, which was given by the corresponding ground-water activity limit, are 11 and 5 mSv/h for a point source (injection) and a distributed source (collimation section), respectively. The red-plot (DS1) in Fig.10, which corresponds to prompt-dose rate at the soil boundary under the sub-tunnel floor, is below 11 mSv/h in the injection region and below 5 mSv/h in the collimation section. More detail is described in Ref. [6].
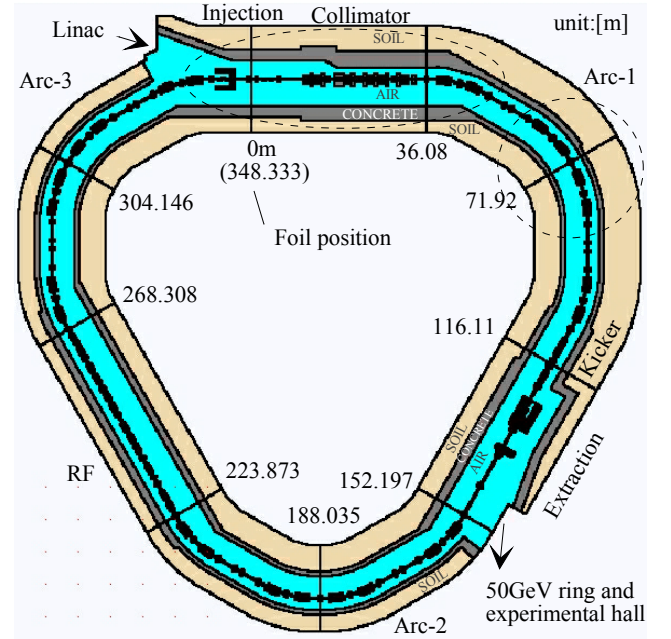

Fig.6. Top view of J-PARC 3GeV-RCS using MMBLB. Marked locations are magnified and shown in Fig.7 and Fig.8 for collimator and arc sections, respectively.
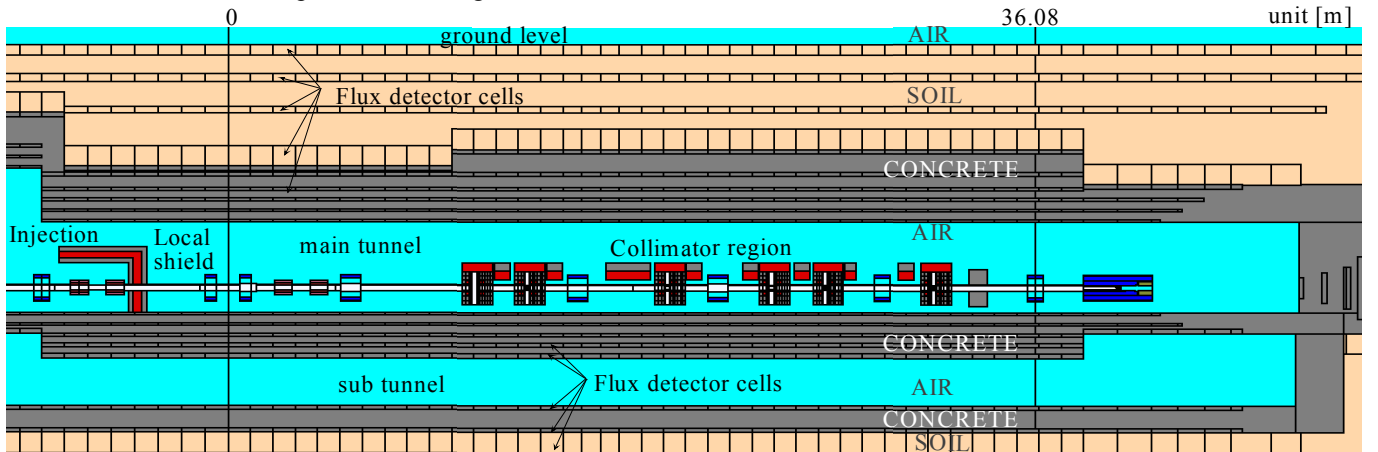

Fig.7. Vertical view of J-PARC 3GeV-RCS from the injection through collimation section. (marked region in Fig.6)
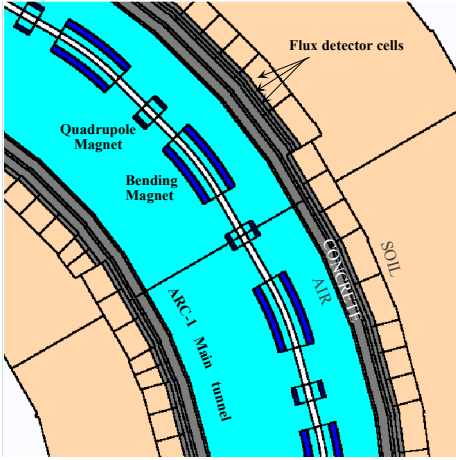
Fig.8. Top view of first arc section with bend-type dipole magnets of J-PARC 3GeV-RCS marked in Fig.6.
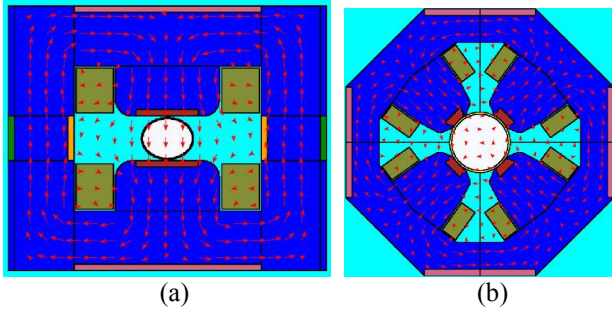

(a)   (b)

Fig.9. Cross-sectional views of and (a)dipole and (b)quadrupole magnets with their magnetic-field images used in J-PARC calculation.
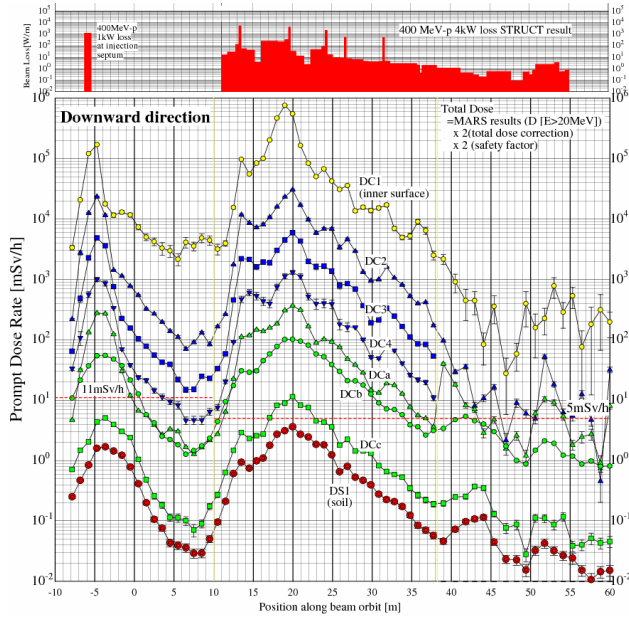

Fig.10. Prompt-dose rate distributions at detector cells shown in Fig.7 in various depths of shielding at floor and sub-tunnel from the injection through collimation section. Source term given by STRCUT result is also shown.

IV. MAIN INJECTOR AND LHC

Fig.11 shows geometry using MMBLB for a 180-m collimation section of the 120-GeV proton Main Injector at Fermilab [10].

Fig.12 shows simulation results for 7-TeV proton LHC at CERN. A 2D color plot for muon flux distribution along the 500-m IP5 bent beam line and tunnel.
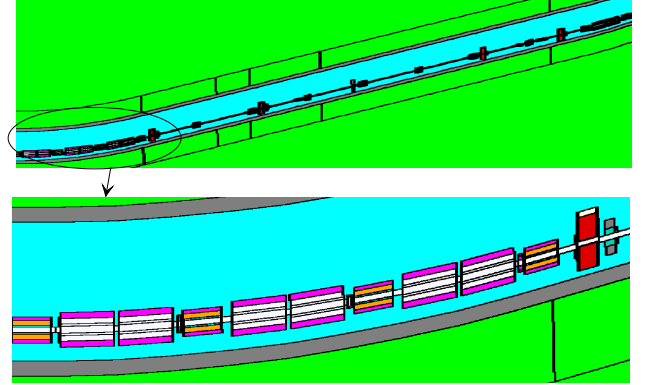

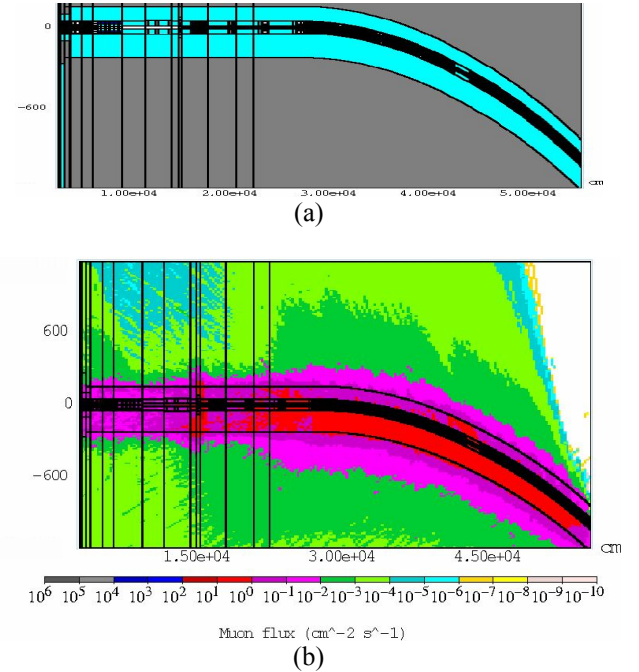Fig.11. Geometry of 180-m collimation section of 120-GeV proton Fermilab Main-Injector using MMBLB.

(a)

Muon flux (cm^-2 s^-1)

(b)

Fig.12. (a) Geometry and (b) muon flux in 2D color plot for 500-m IP5 section for 7-TeV LHC at CERN using MMBLB.

V. ILC BDS

V.A. Overview

MARS15 simulations for the BDS (Beam Delivery System) of the ILC (International Linear Collider) using MMBLB were performed to obtain spatial distributions of primary and secondary particles in the BDS beam line, tunnel, and IR hall.

Suppression of muon background at the IR hall is one of the most important issues for the collider detector performance [11]. Since ILC provides 11 MW electron and positron beams, 0.1% beam loss at BDS causes serious problems for detector background and radiation safety. Using MARS15 code, muon flux at the IR hall was simulated, and muon background suppression was studied with two types of muon-spoiler. Muon flux at the interaction region (IR hall) were compared between MARS15 and MUCARLO code [12], and are reported in Ref.[13].

V.B. Geometry

The BDS beam line from 1.663 km upstream of the interaction point (IP) was described using MMBLB. Fig.13 shows a top view of the BDS tunnel with an entire region of the positron beam line in MARS simulation. The IR hall and the electron beam-dump line are designed at -10 m and -320 m upstream from the IP. Upstream beyond the muon spoiler hall, the tunnel cross section is a cylindrical shape with an inner radius of 2 m with flat floor as shown in Fig.2 (a). Concrete wall of the tunnel is 30-cm thick.

Detailed description of the beam line from PC3 to PDUMP is shown in Fig.14. The beam line consists of beam pipes, dipole, quadrupole magnets, primary collimators (SP), copper protection collimators (PC) (214 mm thick) and copper absorbers (AB) (105-429mm thick). The beam-line height is 75 cm from the floor (57.29 cm below the tunnel-cylinder center) in the entire region. The orbit at -1.663 km is located in the horizontal center of the tunnel.
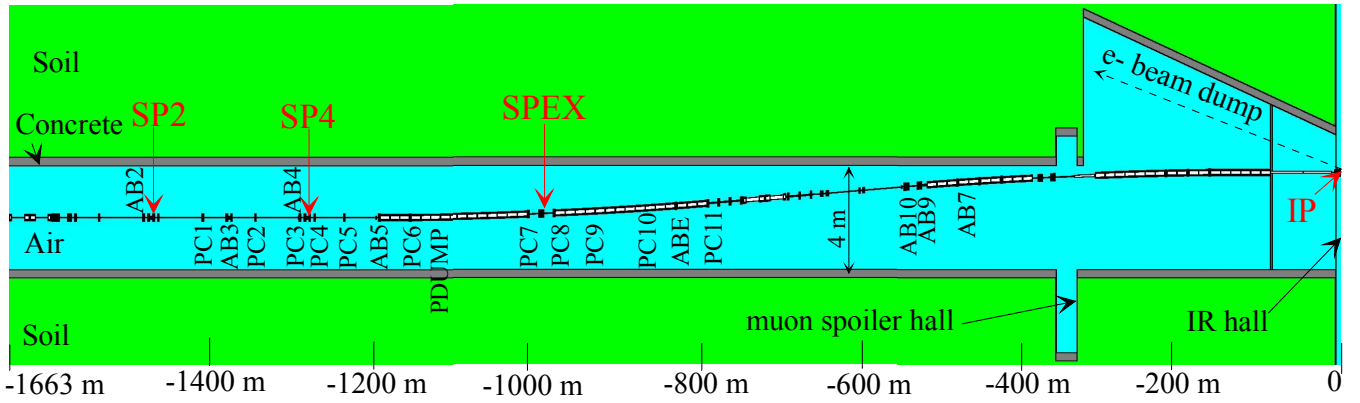

Fig. 13. BDS beam line from interaction point (IP) to 1.663 km upstream described by MMBLB with locations of primary collimators (SP), protection collimators (PC) and absorber (AB).
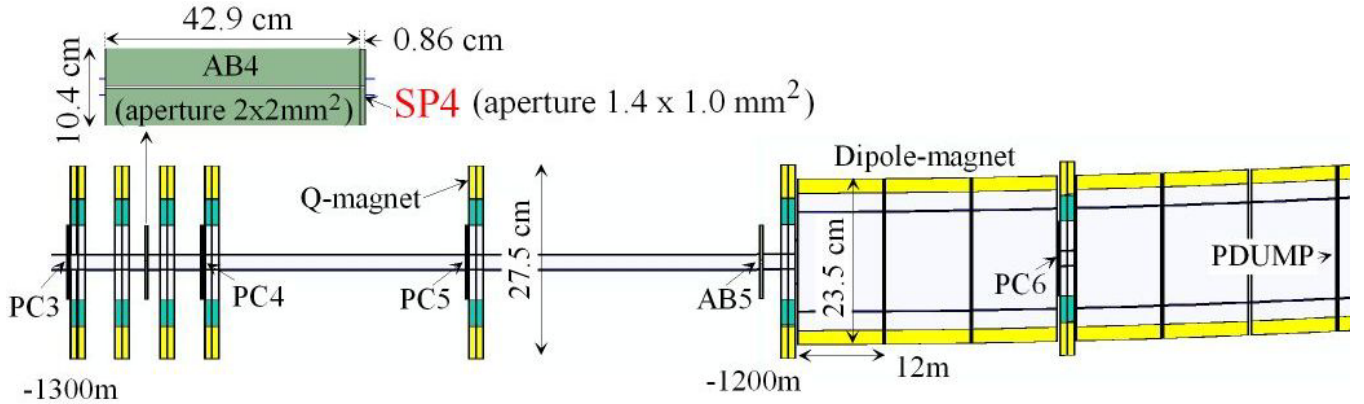

Fig. 14. BDS Beam-line in the region from PC3 to PDUMP. Magnified view of AB4 with SP4 is also shown.

V.C. Muon Spoiler

Two types of muon-spoilers (wall type and donut type) made of iron with magnetic fields are alternatively used to study suppression of the muon background. The wall type, as shown in Fig.15, is 5-m thick covering the tunnel cross section located in a muon-spoiler hall upstream of electron-beam dump line. Muons can be effectively swept because of no muon origins after the wall-spoiler and because of its size and thickness. However, it is costly.

Five donut-type muon-spoilers, shown in Fig.16, are located in the straight section after several protection collimators(PCs), which are the locations of the dominant muon origins. Although one muon-spoiler can be a smaller size in this case, many muon-spoilers are needed to cover most of locations of muon origins.

V.D. Source Term

The beam halo of 250-GeV positron beam in the ILC BDS which was simulated by the STRUCT code [9] was used for the source term of MARS15 simulation. Fig.17 shows beam halo particle at the three primary collimators SP2, SP4 and SPEX with intensity fractions of 35.7%, 42.4% and 21.9%, respectively. The scraping rate is 0.1% of total beam intensity, i.e. 2.82×10^{11} sec^{-1}.

V.E. Beam Tracking Test

Fig.18 shows particle tracks of the first 20 primary positrons (source term) and the produced secondary particles at the copper primary collimator (SP2). It can be seen that positrons in the beam halo of the source term interacted or scattered at the SP2. Even if the positrons went through SPs with a very small angle, they finally interacted at PCs or ABs downstream.

Images of magnetic fields defined in the dipole and quadrupole magnets are shown in Fig.19. These effects were confirmed by the beam tracking test as shown in Fig.20. 250-GeV positrons going through magnetic fields are focused or defocused by quadrupole, and bent by dipole magnet. The center positron beam reaches to the center of IP through the 1633-m beam line.

V.F. Results and discussion

Fig.21 shows two-dimensional distributions of total muon flux for no, wall and donut muon-spoiler cases. From the figures, most of muons are generated in thick collimators such as PCs and ABs, and the muons bent by dipole and quadrupole magnets are penetrating deeply in soil. From Fig.21 (b), the wall muon-spoiler sweeps muons into side soil region quite effectively. From Fig.21(c), on the other hand, although muons generated before the five donut muon-spoilers can be swept

effectively, more donut muon-spoilers are needed also in the bending magnet section where the muon-spoiler can hardly be inserted.

Compared with muon background at the IR hall for no muon-spoiler case, suppressions are about 1/5 and 1/50 for donut and wall muon-spoiler, respectively. Muon-background dependence on the muon-spoiler type at IR hall can clearly be seen also in Fig.21.
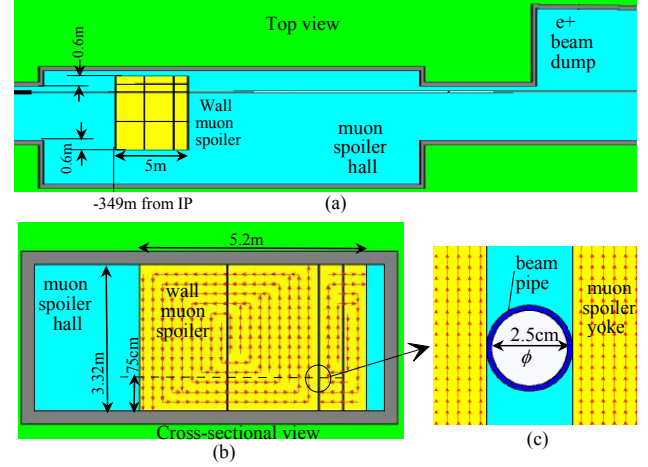

Fig.15. Wall muon spoiler with its dimension and magnetic field image in (a) horizontal plane and (b) (c) cross-sectional plane. Beam direction is from back to front of the figures in (b) and (c).
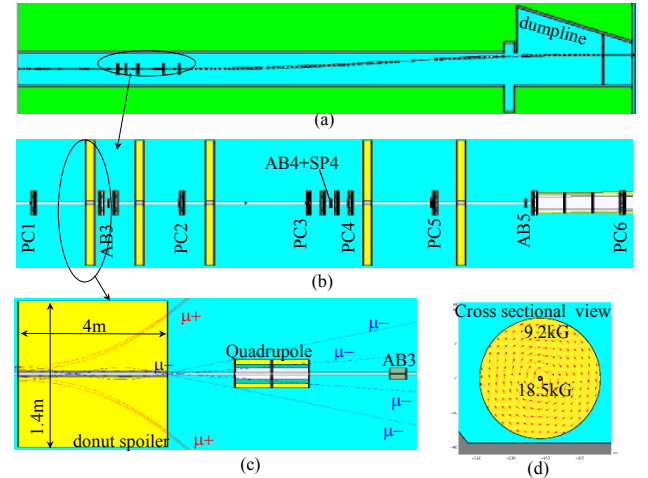

Fig. 16. Donut muon spoilers equipped in the beam line. (a) Locations in the entire beam line, (b) locations in the magnified beam line, (c) image of muon bent by the muon spoiler, and (d) cross-sectional view of the muon spoiler with a magnetic field image. Beam direction is from back to front of the figures in (d).
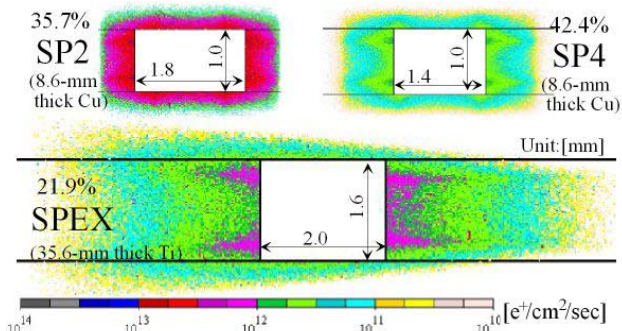
Fig.17. Cross-sectional profiles of the positron beam halos simulated by STRUCT code at the three primary collimators.

Fig.20. Tracing tests of 250-GeV positron beam through magnetic fields of focus, defocus and bending magnet.
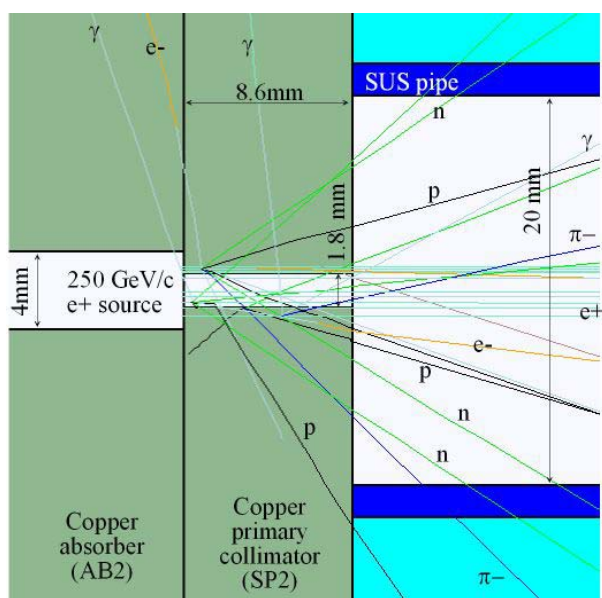

Fig.18. Tracking image of the positron beam halo (source term) and the produced secondary particles at the copper primary collimator (SP2).

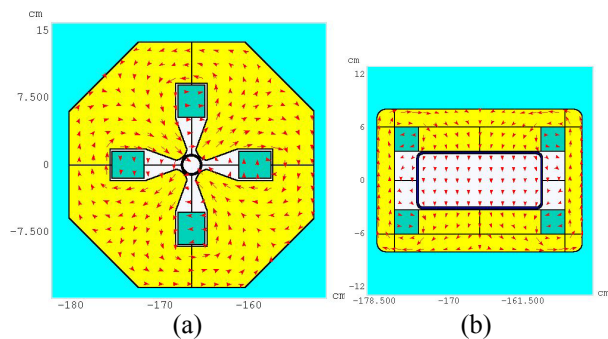Fig.19. Cross-sectional views of (a)quadrupole and (b)dipole magnets with their magnetic-field images used in BDS calculation.
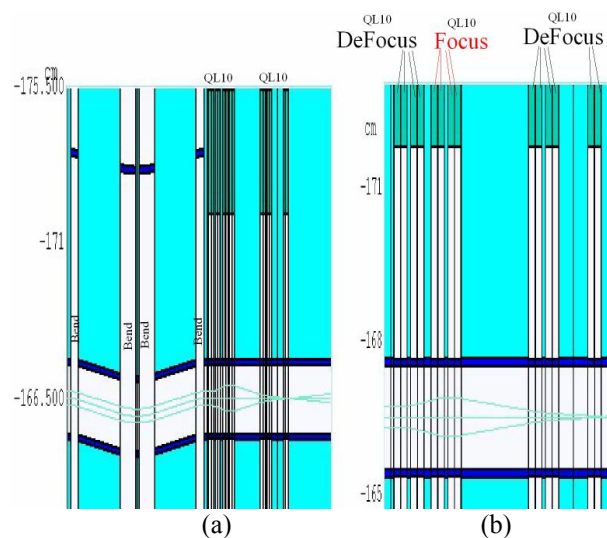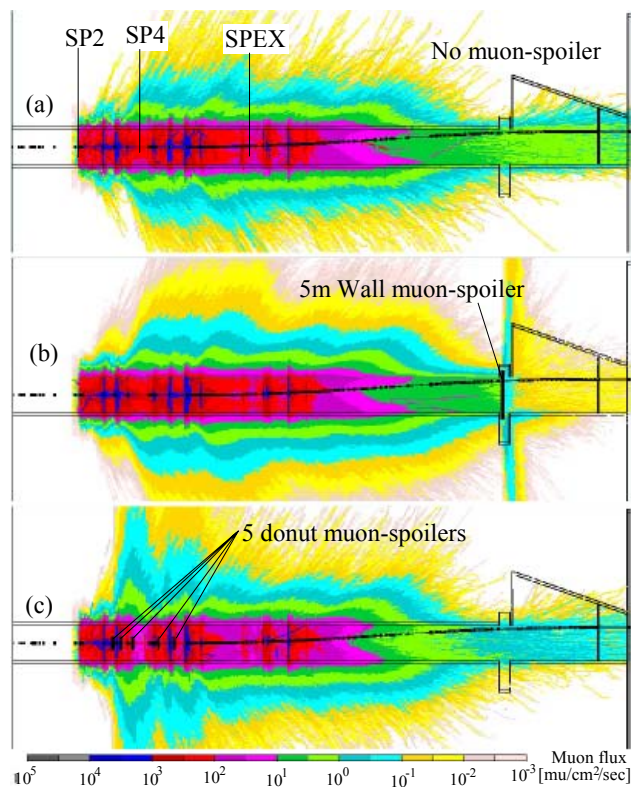

Fig.21. Two-dimensional distributions of total muon flux for (a) no, (b) wall and (c) donut muon-spoiler cases.

ACKNOWLEDGMENTS

REFERENCES

1. N.V. Mokhov, "The MARS Code System User's Guide'", Fermilab-FN-628 (1995); N.V. Mokhov et al, Fermilab-Conf-04/053(2004); http://www-ap.fnal.gov/MARS.
2. D. Mokhov, O.E Krivosheev, E. McCrory, L.F. Ostiguy, "MAD Parsing and Conversion Code", FERMILAB-TM-2115 (2000).
3. O.E. Krivosheev, E. McCrory, L. Michelotti, D. Mokhov, N. Mokhov, J.-F. Ostiguy, "A Lex-based MAD parser and its applications", Proc. IEEE Particle Accelerator Conference (PAC 2001), PAC-2001-RPAH084, pp.3036-3038, Chicago, Illinois, 18-22 Jun 2001; FERMILAB-CONF-01-142-T (2001).
4. M.A. Kostin, O.E. Krivosheev, N.V. Mokhov and I.S. Tropin, "An Improved MAD-MARS Beam Line Builder: User's Guide", FERMILAB-FN-0738-rev (2004).
5. H. Grote and F.C. Iselin, "the MAD program (Methodical Accelerator Design)", CERN/SL/90-13 (1990).
6. N. Nakao, N. Mokhov, K. Yamamoto, Y. Irie and A. Drozhdin, "MARS14 Shielding Calculations for the J-PARC 3 GeV RCS", KEK Report 2004-1 (2004).
7. N. Nakao, N. Mokhov, K. Yamamoto, Y. Irie and A. Drozhdin, "MARS14 Monte Carlo simulation for the shielding studies of the J-PARC 3 GeV ring", *Proc. 10th International Conference on Radiation Shielding (ICRS10)*, Madeira, Portugal, May 9-14, 2004, *Radiat. Prot. Dosim.* Vol.**116**, No.1-4, pp85-88 (2005).
8. J.H. Billen, L.M. Young, "POISSON SUPERFISH", LA-UR-96-1834 (1996).
9. I.S. Baishev, A.I. Drozhdin, N.V. Mokhov, X. Yang, "STRUCT Program User's Reference Manual", http://www-ap.fnal.gov/users/drozhdin.
10. I. Rakhno, "Radiation Shielding for the Main Injector Collimation System", Fermilab-TM-2391-AD(2007).
11. D.S. Denisov et al., JINST 1, P12003 (2006).
12. L. Keller, SLAC-PUB-6385 (1993)
13. A.I. Drozhdin, L. Keller, N.V. Mokhov, N. Nakao, S.I. Striganov, "Suppression of Muon Background Generated in the ILC Beam Delivery System", Proc. 2007 Particle Accelerator Conference (PAC07), Albuquerque, NM, USA, June 25-29, 2007; FERMILAB-CONF-07-276-AD (2007).